Available online at www.sciencedirect.com
ScienceDirect
Journal of Solid State Chemistry 180 (2007) 1990–1997
JOURNAL OF SOLID STATE CHEMISTRY
www.elsevier.com/locate/jssc

Novel KTP-like complex phosphates $KM^{II}_{0.33}Nb_{0.67}PO_5$ (M^{II}—Mn, Co)

A.A. Babaryk[a,*], I.V. Zatovsky[a], V.N. Baumer[b], N.S. Slobodyanik[a], P.G. Nagorny[a], O.V. Shishkin[b]

[a]*Inorganic Chemistry Department, Kiev University, Volodimirska Street 64, Kiev 01033, Ukraine*
[b]*STC "Institute for Single Crystals" NAS of Ukraine, 60 Lenin ave., Kharkiv 61001, Ukraine*

Received 24 January 2007; received in revised form 26 April 2007; accepted 27 April 2007
Available online 6 May 2007

Abstract

Single crystals of KTP-related phosphates of general formula $KM^{II}_{0.33}Nb_{0.67}PO_5$ (M^{II}—Co, Mn) have been obtained in the pseudo-binary system $K_2Mo_2O_7$–$KM^{II}_{0.33}Nb_{0.67}PO_5$ by means of the flux technique. The compounds have been studied by single crystal and powder X-ray diffraction, FTIR and UV–VIS spectroscopy. Both complex phosphates belong to the tetragonal system and crystallize in the enantiomorphous polar space groups $P4_1$ and $P4_3$. The structure contains *cis*-like helical chains which are connected by corner sharing $Nb(M^{II})O_6$ octahedra and further linked through the PO_4 tetrahedra. The potassium cations are located in the channels running along [001] direction of the anionic framework $[M^{II}_{0.33}Nb_{0.67}PO_5]^-$ and are irregularly coordinated by eight oxygen atoms. Potassium atom site is split into two equally occupied positions with $q = 0.5$.

Keywords: Complex phosphates; KTP($KTiOPO_4$)-related compounds; Crystal growth; Crystal structure; FTIR-spectroscopy

1. Introduction

Potassium titanyl phosphate $KTiOPO_4$ (KTP) and complex phosphates of closely related structure are well known due to the nonlinear optical [1–3] and domain ferroelectric properties [4]. From the standpoint of relationship between the structure and properties, the latter could be partially explained by the presence of *cis–trans* alternating −Ti=O–Ti=O metal–oxygen chains. Previously, approaches for the fine-tuning of the KTP properties considered the aliovalent substitution method presuming the replacement of potassium [5–11], titanium [12–18], and phosphorus [11,18–21] atoms.

In particular, partial substitution of titanium atoms by niobium ones leads to improvement of the nonlinear optical properties [12,14,15]. Due to different construction principles of the anionic sublattices $[MOPO_4]$, it is necessary to find out a relationship between the composition and the structure through a systematic exploration of $M^{n+} + Nb^{5+}$ aliovalent substitution in order to develop materials with preprogrammed properties.

In this paper we describe the single crystal structure, FTIR and UV–VIS spectra of new complex phosphates $KM^{II}_{0.33}Nb_{0.67}PO_5$ (M^{II}—Mn, Co). The complex phosphates $KMg_{0.33}Nb_{0.67}PO_5$ [22], $KM^{III}_{0.5}Nb_{0.5}OPO_4$ (M^{III}—V,Fe,Cr) [23,24] were reported earlier.

2. Experimental

2.1. Single crystal preparation

Single crystal samples were obtained by flux method. All the reagents were of analytical grade purity.

For preparation of $KCo_{0.33}Nb_{0.67}PO_5$ 35.28 g KPO_3, 12.07 g $CoCO_3 \cdot Co(OH)_2 \cdot xH_2O$ (containing 59.1% mass. CoO), 26.51 g Nb_2O_5 and 100.0 g $K_2Mo_2O_7$ were mixed and grounded in an agate mortar. Molar ratio Co:Nb:P was kept equal to 1:2:3. The mixture was melted in a 200 ml platinum crucible at 1273 K. Melted solution was cooled at a rate 5 K h^{-1} up to 900 K. The crystals were washed from the rest of the melt components with hot 5%—aqueous ammonia. Common yield was 60.5% (36.3 g).

*Corresponding author.
E-mail address: babaryk@bigmir.net (A.A. Babaryk).

0022-4596/$ - see front matter © 2007 Elsevier Inc. All rights reserved.
doi:10.1016/j.jssc.2007.04.023

Single crystal samples of $KMn_{0.33}Nb_{0.67}PO_5$ were obtained by the following operation sequence: well-grounded mixture of 30.76 g KPO_3, 7.55 g MnO_2 and 23.08 g Nb_2O_5 was placed into a 200 ml platinum crucible, melted at 1273 K and exposed until the gas evolution (due to the MnO_2 decomposition) ceased. The resulting homogenous flux was stirred for 15 min. The 100.0 g of dispersed $K_2Mo_2O_7$ was added, the flux was stirred for additional 5 min and exposed at the same temperature for 2 h. The cooling and washing processes were as for the above preparation. Common yield was 68.8% (41.27 g).

Both the compounds form faceted square-bipyramidal crystals (Fig. 1). Fractional compositions at spontaneous crystallization conditions are presented in Table 1.

Evaluation of the elements quantities was performed on an X-ray fluorescence energy dispersive spectrometer "Elvax Light". Compositions of the crystalline products were refined and established by ICP determination performed on a "Spectroflame Modula ICP" instrument. The element ratio 3:1:2:3 was evidenced.

2.2. X-ray data collection and structure solution

The X-ray diffraction pattern was collected using an automated diffractometer Siemens D500 operating in a Bragg–Brentano ($\theta/2\theta$) geometry (Cu$K\alpha$ radiation, $\lambda = 1.54184$ Å; curved graphite monochromator on the counter arm; step size 0.02°; scanning rate 10 s/point). The samples were gently grounded in an agate mortar and the data were collected at room temperature over the 2θ angular range of 5–85°.

Single-crystal X-ray diffraction measurements were performed using crystals of dimensions given in Table 2. The intensity data were collected with an φ–ω-scan technique ($\Delta\omega = 1.0°$). The exposure time was 25 s/image. The 2048 × 2048 images were taken in eight sets at different φ and ω positions and covered about 99.8% of the Ewald sphere. The intensities were integrated and corrected for Lorentz polarization [25]. Twinning was not detected in the process of the diffraction experiments treatment. The structures were solved with direct methods using the SHELXS-97 program [26]. The structure refinement

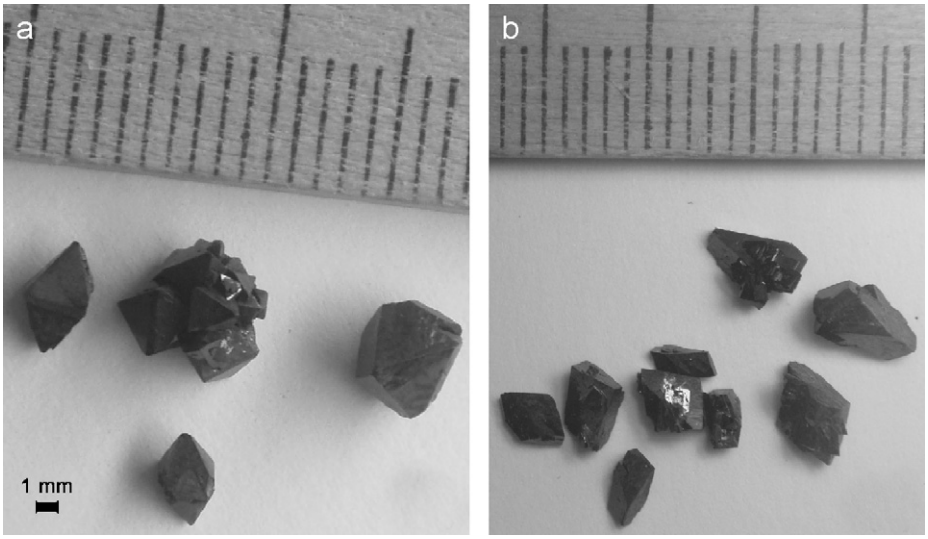

Fig. 1. View of $KMn_{0.33}Nb_{0.67}PO_5$ (a) and $KCo_{0.33}Nb_{0.67}PO_5$ (b) crystalline samples.

Table 1
Fractional compositions for $KMn_{0.33}Nb_{0.67}PO_5$ and $KCo_{0.33}Nb_{0.67}PO_5$ in spontaneous crystallization conditions

Compound	Color	Common yield (g)	Resulting fractions (g/% wt.)				
			Maximal size (mm)				
			<3.0	3.0–2.0	2.0–1.0	1.0–0.5	>0.5
$KCo_{0.33}Nb_{0.67}PO_5$	Violet	36.30	7.37/20.3[a]	3.50/9.7	6.47/17.8	4.72/13.0	14.24/39.2
$KMn_{0.33}Nb_{0.67}PO_5$	Brown	41.27		15.02/36.4	4.65/11.3	5.20/12.6	16.40/39.7[b]

[a]A large fracture space.
[b]Contain < 10% wt. of $K_6MnNb_7P_5O_{34}$.

Table 2
Crystal data and refinement of $KMn_{0.33}Nb_{0.67}PO_5$ and $KCo_{0.33}Nb_{0.67}PO_5$

	$KMn_{0.33}Nb_{0.67}PO_5$	$KCo_{0.33}Nb_{0.67}PO_5$
Crystal data		
Crystal system	Tetragonal	Tetragonal
Space group	$P4_1$	$P4_3$
Cell parameter (Å)		
a	6.56530(10)	6.5564(4)
c	10.8311(3)	10.8579(9)
V (Å^3)	466.855 (16)	466.74 (6)
Z	4	4
ρ_{calc} (g/cm^3)	3.277	3.297
Crystal size (mm)	$0.12\times0.07\times0.05$	$0.1\times0.1\times0.1$
Data collection		
Measurement device	Xcalibur Sapphire 3 CCD	Xcalibur Sapphire 3 CCD
Wavelength (Å)	0.71073	0.71073
Monochromator	Graphite	Graphite
Temperature (K)	293(2)	293(2)
Scan mode	φ and ω scans	φ and ω scans
μ (mm^{-1})	3.812	4.095
Absorption correction[a]	Multi-scan	Multi-scan
T_{min}, T_{max}	0.659, 0.833	0.5901, 0.6242
Number of reflections	19441	8614
Number of independent	1353	1346
reflection with $I > 2\sigma(I)$	1317	1342
R_{int}	0.052	0.047
Theta max. (°)	30.0	30.0
$h =$, $k =$, $l =$	$-9\rightarrow9$; $-9\rightarrow9$; $-15\rightarrow15$	$-9\rightarrow9$; $-6\rightarrow9$; $-15\rightarrow15$
$F(000)$	438.7	441.4
Solution and refinement		
Primary solution method	Direct	Direct
Weighting scheme	$w = 1/[\sigma^2(F_o^2)+(0.P)^2+3.1709P]$ where $P=(F_o^2+2F_c^2)/3$	$w = 1/[\sigma^2(F_o^2)+(0.0279P)^2+2.0418P]$ where $P=(F_o^2+2F_c^2)/3$
R_1(all)	0.041	0.031
wR_2	0.077	0.071
S	1.18	1.06
Number of parameters	87	87
Number of restraints	4	4
Extinction coefficient[b]	0.0056 (10)	0.0089 (15)
$(\Delta\rho)_{max,\ min}$ (e Å^{-3})	1.30, −1.03	1.25, −0.93
Flack parameter[c]	0.10(10)	0.09(6)

[a]R.H. Blessing, Acta Crystallogr. A51 (1995) 33–38.
[b]See Ref. [27].
[c]H. D. Flack, Acta Crystallogr. A39 (1983) 876–881.

calculations were performed with SHELXL-97 program [27]. Coordinates of manganese (cobalt) and niobium atoms and their anisotropic displacement parameters were restrained during crystal structure refinement according to the slight disorder. Crystal data and further experimental details are summarized in Table 2 together with the parameters of the structure refinements. The coordinates and U_{eq} of the atoms are listed in Table 3. The bond lengths and bond angles in the coordination polyhedra are listed in Table 4.

Further details concerning to $KCo_{0.33}Nb_{0.67}PO_5$, $KMn_{0.33}Nb_{0.67}PO_5$ crystal structure investigations are available from the Fachinformationszentrum Karlsruhe, D-76344 Eggeinstein-Leopoldshafen (Germany), on quoting the depository numbers CSD-417461 and CSD-417462.

2.3. FTIR and UV–VIS measurements

FTIR spectra were collected with a NICOLET Nexus 470 FTIR spectrometer (KBr pellets; the spectral range 400–4000 cm^{-1}; spectral resolution 0.5 cm^{-1}). UV–VIS spectra were registered with a Specord-40 automatic PC controlled spectrometer operating in a diffuse scattering mode (frequency limits 12000–38500 cm^{-1}).

3. Results and discussion

3.1. Phase formation in pseudo-binary system $K_2Mo_2O_7$–$KM^{II}_{0.33}Nb_{0.67}PO_5$ (M^{II}—Mn, Co)

Recently it was shown that tungstate and molybdate fluxes are suitable for $KTiOPO_4$ single crystal growth due to their low volatility and low viscosity, faster dissolution kinetics than those of pure phosphate melts and also due to a high quality of the resulting crystalline samples [28]. Potassium dimolybdate fluxes have some advantages as media for the single crystal growth: (1) pure $K_2Mo_2O_7$ melts congruently at sufficiently low temperature (748 K); (2) it possesses a high dissolving ability. These reasons stimulated us to apply $K_2Mo_2O_7$ as a high temperature solvent.

All the experiments were carried out in a pseudo-binary system $K_2Mo_2O_7$–$KM^{II}_{0.33}Nb_{0.67}PO_5$ (M^{II}—Mn, Co). Molar ratios between potassium metaphosphate and metal oxides were chosen basing on the principle of aliovalent pair combination $Ti^{4+}\rightarrow0.33M^{2+}+0.66Nb^{5+}$. Reagent mixture to solvent weight ratio was from 2:10 to 6:10.

As it was expected the final temperature of the crystallization was rather low and lay in a range of 898–923 K.

Furthermore, in $K_2Mo_2O_7$–$KMn^{II}_{0.33}Nb_{0.67}PO_5$ system at high concentrations the crystallization of the target product was accompanied by the additional phase $K_6MnNb_7P_5O_{34}$ below 913 K. According to the X-ray powder data (Fig. 2), the amount of the latter compound does not exceed 10% weight of the least crystalline fraction (Table 1). This complex phosphate is isostructural to $K_4Nb_8P_5O_{34}$ [29] and it belongs to a family of closely related compounds $K_5Zr_2Nb_6P_5O_{34}$ [30], $K_{5,84}Ti_{2,848}Nb_{5,152}P_5O_{34}$ [31] and $K_{2.47}Nb_{2.85}Ti_{1.15}P_{2.5}O_{17}$ [32]. Such feature of the interaction was not detected for $K_2Mo_2O_7$–$KCo^{II}_{0.33}Nb_{0.67}PO_5$ system that could be explained by a wider liquidus range.

Pure crystalline products $KMn_{0.33}Nb_{0.67}PO_5$ could be extracted by sieving into the fractions starting from 0.5 mm.

Table 3
Atomic coordinates and Ueq for $KMn_{0.33}Nb_{0.67}PO_5$ (in $P4_1$) and $KCo_{0.33}Nb_{0.67}PO_5$ (in $P4_3$)

Atom	Site	Occ.	*x*	*y*	*z*	*U*eq
$KMn_{0.33}Nb0.6_7PO_5$[a]						
Nb1/Mn1	4*a*	0.6594(1)/0.3406(2)	0.50000(8)	0.74256(9)	0.96913(10)	0.02062(15)
K1	4*a*	0.436(4)	0.2293(11)	0.7871(9)	0.5285(5)	0.068(2)
K2	4*a*	0.564(4)	0.2033(9)	0.7845(11)	0.6474(7)	0.114(3)
P1	4*a*		1.00006(18)	0.65407(19)	0.9690(2)	0.0190(3)
O1	4*a*		0.9700(10)	0.5181(9)	0.8538(6)	0.0371(17)
O2	4*a*		0.5180(9)	0.9730(10)	0.8310(7)	0.042(2)
O3	4*a*		0.8120(7)	0.7866(7)	0.9913(4)	0.0279(10)
O4	4*a*		0.1863(7)	0.7873(7)	0.9475(5)	0.0276(10)
O5	4*a*		0.5438(8)	0.5421(8)	0.8461(5)	0.0234(9)
$KCo_{0.33}Nb_{0.67}PO_5$[a]						
Nb1/Co1	4*a*	0.66670(10)/ 0.3333(2)	0.00007(6)	0.75611(6)	0.13204(6)	0.01581(12)
K1	4*a*	0.460(4)	0.2676(8)	0.7153(7)	0.5828(4)	0.0636(15)
K2	4*a*	0.540(4)	0.2893(7)	0.7251(10)	0.4371(5)	0.0902(19)
P1	4*a*		0.50007(14)	0.84675(14)	0.13201(13)	0.01133(18)
O1	4*a*		0.5310(8)	0.9852(6)	0.2458(4)	0.0210(9)
O2	4*a*		0.0425(6)	0.9570(6)	0.0055(4)	0.0174(6)
O3	4*a*		0.6905(5)	0.7142(5)	0.1108(3)	0.0187(7)
O4	4*a*		0.3119(5)	0.7135(6)	0.1528(3)	0.0201(7)
O5	4*a*		0.4729(7)	0.9853(6)	0.0185(4)	0.0214(9)

[a]Atom site occupancies and corresponding e.s.d. obtained due to free variables liner restraints. See Ref. [27].

3.2. Crystal structure

The structures of $KM^{II}_{0.33}Nb_{0.67}PO_5$ (M^{II}—Mn, Co) belong to a group of KTP-related phosphates. They occur to be non-centrosymmetric and crystallize in $P4_1$ and $P4_3$ space groups with the lattice parameters given in Table 3. The asymmetric unit consists of 9 independent atoms, all of which reside in general positions.

Either niobium, manganese or cobalt atoms were surrounded by six oxygen atoms providing distorted octahedral environments. All $Nb(M^{II})O_6$ octahedra are linked via common oxygen vertices forming *cis*-like type helical chains stretching along [001] direction (Fig. 3). Two bonds $Nb(M^{II})$–O participating in the –O–$Nb(M^{II})$–O–$Nb(M^{II})$– chain formation are shortened and spread in the range 1.896(5)–1.916(5) Å (Table 4). The dispersion of bond angles O–$Nb(M^{II})$–O is found within the limits of 82.67(15)–99.7(2) and 163.97(16)–174.6(2) exhibiting a slightly distorted type of $Nb(M^{II})O_6$ octahedrons.

Each PO_4 tetrahedron interconnects two independent chains into the three-dimensional framework via common vertices. Local symmetry of PO_4 tetrahedron is C_1. The interatomic distances and angles are actually typical [33], with characteristic P–O separations: distances P–O and O–P–O angles are spread in the range 1.516(7)–1.554(4) Å and 107.6(3)–111.6(3)° subsequently.

The anionic framework $[M^{II}_{0.33}Nb_{0.67}PO_5]^-$ is intersected by a system of the channels stretching along *c*-axis which provide a space for situation of potassium cations (Fig. 4). Comparatively large ADPs of potassium atoms may be explained by thermal movements in the oxygen cavities. The potassium cations are irregularly coordinated by eight O atoms (Fig. 5) assuming a cut-off distance of 3.35 Å (the next-closest K–O contacts are 3.438(8) Å for $KMn_{0.33}Nb_{0.67}PO_5$ and 3.463(7) Å for $KCo_{0.33}Nb_{0.67}PO_5$, respectively). Thus the present K–O bond lengths vary starting from 2.608(9) Å (typical ionic bonds) up to 3.286(7) Å (long contacts) (Table 4).

In both structures, the potassium atom positions are split on two equally occupied ones with $q = 0.5$ and consequent K1–K2 contact is 1.299(7) Å for $KMn_{0.33}Nb_{0.67}PO_5$ and 1.589(5) Å for $KCo_{0.33}Nb_{0.67}PO_5$. The nearest contacts between two couples of equal K1–K2 position are 3.248(7) and 3.206(7) Å in cavities running along the *c* direction.

cis-Linkage of the metal-oxygen chains is detected for aliovalent KTP-related structures $KMg_{0.33}Nb_{0.67}PO_5$ [22], $K_2MgWO_2(PO_4)_2$ [34], $K_2NiWO_2(PO_4)_2$ [35] as well as for isovalent ones β-$NaTiOPO_4$ [36] and $RbIn(OH)PO_4$ [37]. Structure of the titled compounds is built up similar to the previously reported $KMg_{0.33}Nb_{0.67}PO_5$ (Space group $P4_322$ no. 95, $a = 6.535(1)$, $c = 10.841(2)$ Å, $Z = 4$) [22]. The niobium and manganese (cobalt) atoms are equally redistributed on two independent positions in $KM^{II}_{0.33}Nb_{0.67}PO_5$ (M^{II}—Mn, Co), while in $K_2MgWO_2(PO_4)_2$ and $K_2NiWO_2(PO_4)_2$ each site was occupied by definite atom type.

During the structure refinements the independent K1 and K2 atom positions were found as separate peaks from the Fourier difference map. Occupancies of the sites were included to the charge restraints of the cation part using SUMP command [27]. K1 and K2 positions could be

Table 4
Selected bond distances (Å) and angles (deg) for $KMn_{0.33}Nb_{0.67}PO_5$ and $KCo_{0.33}Nb_{0.67}PO_5$

$KMn_{0.33}Nb_{0.67}PO_5$		$KCo_{0.33}Nb_{0.67}PO_5$	
Nb1/Mn1–O5	1.895(6)	Nb1/Co1–O2^{ii}	1.902(4)
Nb1/Mn1–O5^{ix}	1.916(6)	Nb1/Co1–O2	1.924(4)
Nb1/Mn1–O3	2.082(5)	Nb1/Co1–O3^{viii}	2.061(3)
Nb1/Mn1–O1^{ix}	2.091(6)	Nb1/Co1–O4	2.076(3)
Nb1/Mn1–O4	2.093(5)	Nb1/Co1–O1^{ix}	2.092(5)
Nb1/Mn1–O2	2.131(7)	Nb1/Co1–O5^{ii}	2.112(5)
P1–O1	1.547(6)	P1–O4	1.528(4)
P1–O3	1.530(4)	P1–O3	1.538(3)
P1–O2^{x}	1.516(7)	P1–O5	1.541(4)
P1–O4^{xi}	1.522(5)	P1–O1	1.546(4)
O5–Nb1/Mn1–O5^{ix}	93.07(14)	O2^{ii}–Nb1/Co1–O2	92.84(10)
O5–Nb1/Mn1–O3	91.62(19)	O2^{ii}–Nb1/Co1–O3^{viii}	91.44(14)
O5^{ix}–Nb1/Mn1–O3	98.8(2)	O2–Nb1/Co1–O3^{viii}	98.86(16)
O5–Nb1/Mn1–O1^{ix}	174.4(2)	O2^{ii}–Nb1/Co1–O4	99.38(17)
O5^{ix}–Nb1/Mn1–O1^{ix}	88.7(3)	O2–Nb1/Co1–O4	91.55(15)
O3–Nb1/Mn1–O1^{ix}	82.9(2)	O3^{viii}–Nb1/Co1–O4	164.60(12)
O5–Nb1/Mn1–O4	99.7(2)	O2^{ii}–Nb1/Co1–O1^{ix}	174.10(17)
O5^{ix}–Nb1/Mn1–O4	91.9(2)	O2–Nb1/Co1–O1^{ix}	88.4(2)
O3–Nb1/Mn1–O4	163.94(16)	O3^{viii}–Nb1/Co1–O1^{ix}	82.66(15)
O1^{ix}–Nb1/Mn1–O4	85.5(2)	O4–Nb1/Co1–O1^{ix}	86.36(15)
O5–Nb1/Mn1–O2	89.5(3)	O2^{ii}–Nb1/Co1–O5^{ii}	89.6(2)
O5^{ix}–Nb1/Mn1–O2	174.6(2)	O2–Nb1/Co1–O5^{ii}	174.10(16)
O3–Nb1/Mn1–O2	85.8(2)	O3^{viii}–Nb1/Co1–O5^{ii}	86.46(15)
O1^{ix}–Nb1/Mn1–O2	89.20(19)	O4–Nb1/Co1–O5^{ii}	82.73(15)
O4–Nb1/Mn1–O2	82.9(2)	O1^{ix}–Nb1/Co1–O5^{ii}	89.81(11)
O2^{x}–P1–O4^{xi}	111.5(3)	O4–P1–O3	110.74(17)
O2^{x}–P1–O3	107.7(4)	O4–P1–O5	111.2(2)
O4^{xi}–P1–O3	110.2(2)	O3–P1–O5	107.9(2)
O2^{x}–P1–O1	108.7(3)	O4–P1–O1	108.9(3)
O4^{xi}–P1–O1	108.1(4)	O3–P1–O1	110.2(2)
O3–P1–O1	110.6(3)	O5–P1–O1	107.94(19)
K1–O1^{ii}	2.608(8)	K1–O1^{ii}	2.632(6)
K1–O2^{iii}	2.677(8)	K1–O5^{iii}	2.690(6)
K1–O3^{iv}	2.840(8)	K1–O3^{iv}	2.846(6)
K1–O1^{v}	3.051(9)	K1–O1^{iii}	2.955(6)
K1–O5^{vi}	3.078(8)	K1–O3^{v}	3.026(5)
K1–O3^{vii}	3.117(8)	K1–O5^{v}	3.057(6)
K1–O2^{iv}	3.132(9)	K1–O2^{vi}	3.075(6)
K1–O5^{v}	3.285(11)	K1–O2^{vii}	3.207(8)
K2–O2^{iii}	2.598(7)	K2–O5^{iii}	2.611(6)
K2–O1^{ii}	2.663(7)	K2–O1^{ii}	2.683(6)
K2–O4^{iii}	2.791(8)	K2–O4^{i}	2.816(6)
K2–O2	3.123(10)	K2–O5^{ii}	3.002(6)
K2–O5^{vi}	3.147(8)	K2–O4	3.092(6)
K2–O1^{viii}	3.226(10)	K2–O2^{vi}	3.103(7)
K2–O4	3.253(9)	K2–O1	3.120(7)
K2–O3^{iv}	3.286(10)	K2–O2^{ii}	3.311(9)

Symmetry transformations used to generate equivalent atoms for $KMn_{0.33}Nb_{0.67}PO_5$: (ii) y, $2-x$, $-0.25+z$; (iii) $-1+y$, $1-x$, $-0.25+z$; (iv) $1-x$, $2-y$, $-0.5+z$; (v) $1-x$, $1-y$, $-0.5+z$; (vi) y, $1-x$, $-0.25+z$; (vii) $1-y$, x, $-0.75+z$; (viii) $-1+x$, y, z; (ix) $1-y$, x, $0.25+z$; (x) $2-y$, x, $0.25+z$; (xi) $1+x$, y, z.

Symmetry transformations used to generate equivalent atoms for $KCo_{0.33}Nb_{0.67}PO_5$: (ii) $-1+y$, $1-x$, $0.25+z$; (iii) $1-x$, $2-y$, $0.5+z$; (iv) $1-x$, $1-y$, $0.5+z$; (v) $1-y$, x, $0.75+z$; (vi) $-x$, $2-y$, $0.5+z$; (vii) $1-y$, $1+x$, $0.75+z$; (viii) $-1+x$, y, z; (ix) $1-y$, x, $-0.25+z$.

considered as split ones opposite to the fact of a single half-occupied potassium position which is observed in $KMg_{0.33}Nb_{0.67}PO_5$. Such splitting was detected for other

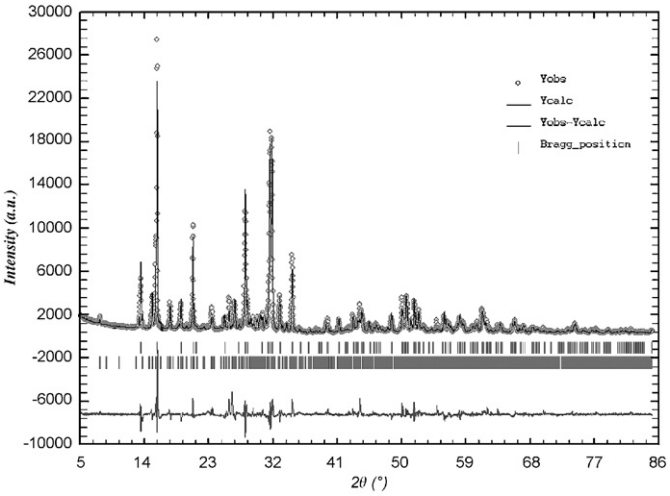

Fig. 2. Powder X-ray diffraction pattern for mixture of $KMn_{0.33}Nb_{0.67}PO_5$ and $K_6MnNb_7P_5O_{34}$ (for >0.5 mm crystalline fraction sample). Circle signs correspond to observed data; the solid line is the calculated profile. Tick marks represent the positions of allowed reflections, and a difference curve on the same scale is plotted at the bottom of the pattern.

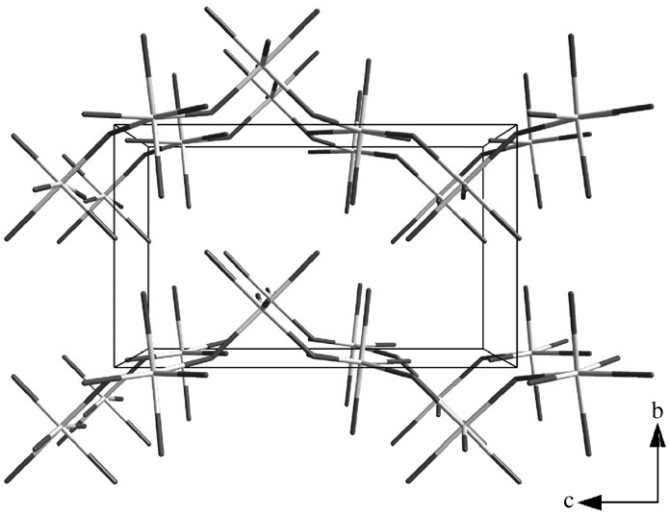

Fig. 3. *cis*-Like type of –O–Nb(M^{II})–O–Nb(M^{II})– chains stretching along [001] directions in $KM^{II}_{0.33}Nb_{0.67}PO_5$ (M^{II}—Mn, Co).

niobium containing KTP-analogues $KM^{III}_{0.5}Nb_{0.5}OPO_4$ (M^{III}—Fe, Cr) [24] and recently was shown also for $KTiOPO_4$ [38] applying synchrotron structure investigations. No usual signs of twinning was detected during the structure refinements [27] that could point out to slight structure distortions in whole.

3.3. FTIR-spectra interpretation

The FTIR spectra of the titled compounds and $KTiOPO_4$ are shown in Fig. 6. The absorption bands confirm simultaneous presence of the phosphate [PO_4]

tetrahedron and [Nb(M^{II})O_6] octahedron groups. By assuming separation of the vibrations into internal and external modes, the following internal modes could be expected for PO_4 anion. Thus, we define ν_1–A_1 and ν_3, ν_4–$A_1+B_1+B_2$ for the IR active stretching vibrations, and ν_2–A_1 and for the bending vibrations.

Set and location of IR absorption bands are almost identical for $KMn_{0.33}Nb_{0.67}PO_5$ and $KCo_{0.33}Nb_{0.67}PO_5$. The bands corresponding to the ν_{as} and ν_s vibration of P–O bonds in PO_4^{3-} tetrahedron are observed at 750–1150 cm^{-1}. All bands in high wave number part of the spectra are rather widen and their number is less due to the increase of lattice symmetry (4/m) comparatively to the $KTiOPO_4$ ($mm2$). Middle strength band at 720 cm^{-1} is present due to the high energy vibrations of shortened Nb(Mn or Co)–O bond while the same band corresponding to vibration of Ti=O fragment is observed at 705 cm^{-1} in $KTiOPO_4$ (Fig. 6). Frequency region 400–700 cm^{-1} contains bands originating in superposition of [Nb(Mn,Co)O_6] octahedra and [PO_4] tetrahedra deformational vibrations (Fig. 6).

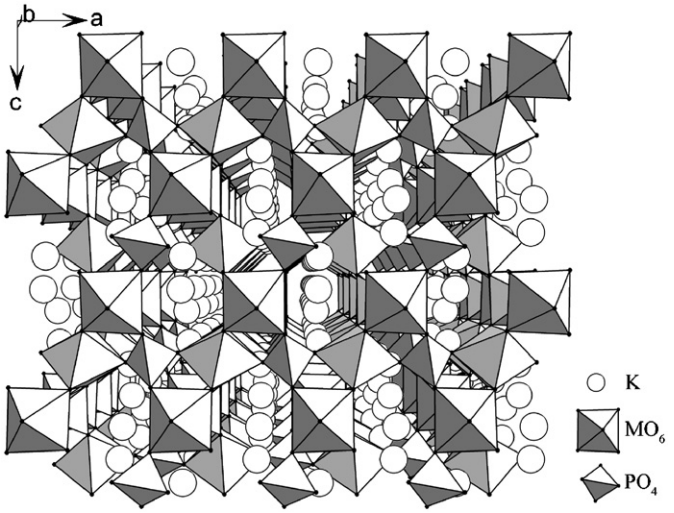

Fig. 4. Potassium ions located in anionic framework $[M^{II}_{0.33}Nb_{0.67}PO_5]^-$ cavities (M^{II}—Mn, Co).

3.4. Electronic spectroscopy

Diffuse scattering electronic spectra of $KCo_{0.33}Nb_{0.67}PO_5$ are characterized by a presence of two wide bands with corresponding frequency values 14 000 and 18 000 cm^{-1} (Fig. 7). Transition bands positions and their intensities show six-coordinated high spin Co(II) configuration in the [CoO_6] chromophore [39]. Band at 18 000 cm^{-1} could be assigned to $^4T_{1g}(P)\rightarrow{}^4T_{1g}$. Its broadening was mainly connected with an admixing of spin prohibited transitions from ^{2}G and ^{2}H states. Transition $^4A_{2g}\rightarrow{}^4T_{1g}$ appears as a

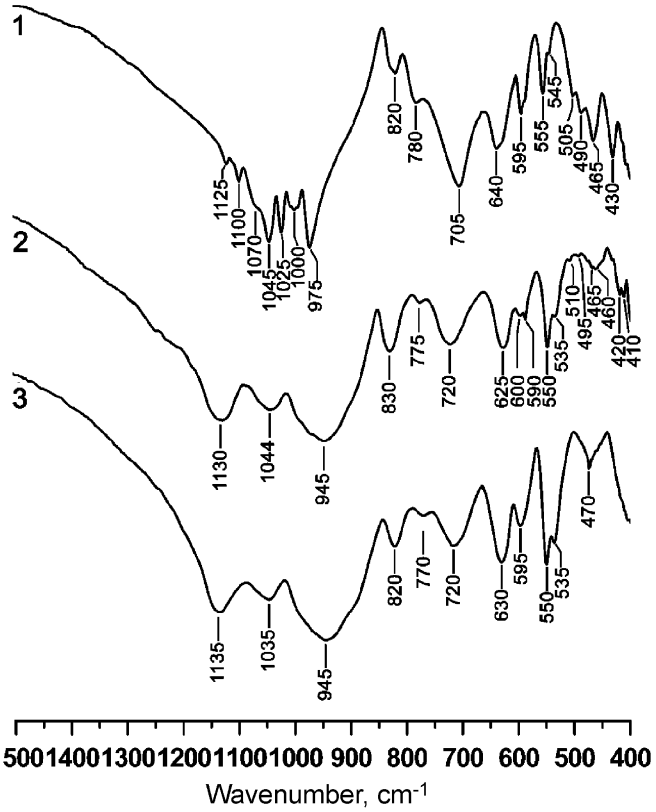

Fig. 6. FTIR-spectra of $KTiOPO_4$ (1), $KMn_{0.33}Nb_{0.67}PO_5$ (2) and $KCo_{0.33}Nb_{0.67}PO_5$ (3).

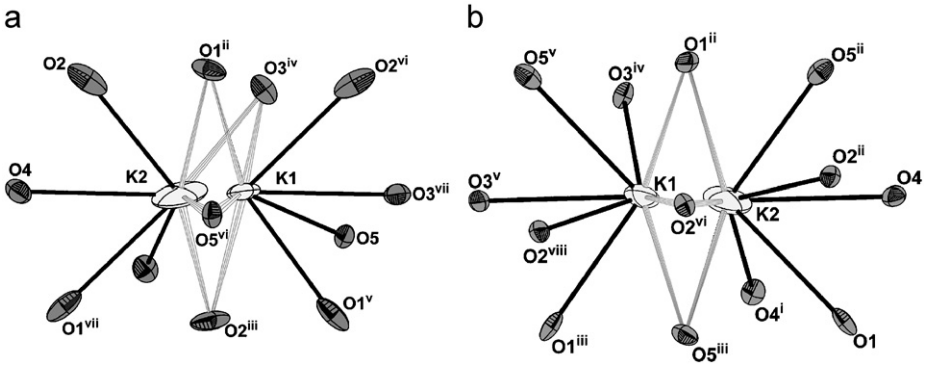

Fig. 5. The oxygen atom coordination around the potassium atoms for $KMn_{0.33}Nb_{0.67}PO_5$ (a) and $KCo_{0.33}Nb_{0.67}PO_5$ (b). Common bonds for both potassium atoms are drawn by multiple stripes (symmetry code: (v) y, $2-x$, $-1/4+z$; (vi) $1-y$, $1+x$, $1/4+z$; (vii) i, $1+y$, z; (viii) $-1+y$, $2-x$, $-1/4+z$; (x) $2-y$, $1+x$, $-1/4+z$; (xi) $1-x$, $2-y$, $-1/2+z$; (xii) $2-y$, x, $-1/4+z$; (xiii) y, $1-x$, $1/4+z$; (xiv) $1+x$, y, z).

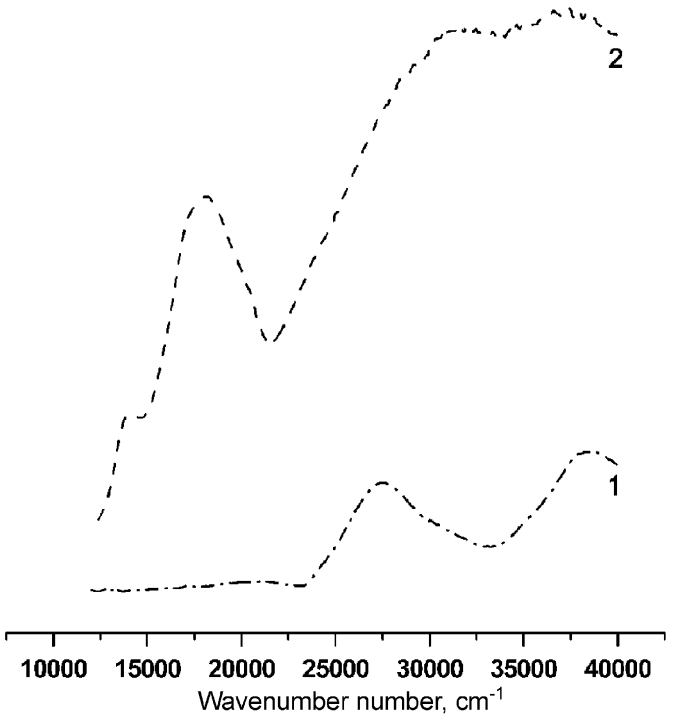

Fig. 7. UV–VIS spectra of $KMn_{0.33}Nb_{0.67}PO_5$ (1) and $KCo_{0.33}Nb_{0.67}PO_5$ (2).

less intensive band at 14 000 cm^{-1}. Attribution of absorption bands for $KMn_{0.33}Nb_{0.67}PO_5$ is bothered due to high extinction coefficient of the samples in a visible part of spectrum (Fig. 7). Two strong well resolved bands confirm $O^{2-} \rightarrow Nb^{5+}$ and $O^{2-} \rightarrow Mn^{2+}$ ($O^{2-} \rightarrow Co^{2+}$) charge transition at 38 500 and 27 500 cm^{-1} (31 500 cm^{-1}).

4. Conclusion

Thus two novel KTP-related complex phosphates $KM^{II}_{0.33}Nb_{0.67}PO_5$ (M^{II}—Mn, Co) were obtained and characterized by powder X-ray diffraction, single-crystal X-ray diffraction, FTIR and electronic spectroscopy studies. Present work demonstrates utility of the $K_2Mo_2O_7$ based melts for synthesis and crystal growth of aliovalent substituted phosphates of KTP family.

Acknowledgments

The authors acknowledge the ICDD for financial support (Grant #03-02).

References

[1] F.C. Zumsteg, J.D. Bierlein, T.E. Gier, J. Appl. Phys. 47 (1976) 4980–4985.
[2] M.N. Satyanarayan, A.N. Deepthy, H.L. Bhat, Crit. Rev. Solid State Mater. Sci. 24 (1999) 103–189.
[3] G.D. Stucky, M.L.F. Phillips, T.E. Gier, Chem. Mater. 1 (1989) 492–509.
[4] C. Canalias, Domain engineering in $KTiOPO_4$, Doctoral Thesis Laser Physics and Quantum Optics Royal Institute of Technology, Stockholm, 2005, pp. 1–108.
[5] V.I. Voronkova, E.S. Shubentsova, V.K. Yanovskii, Inorg. Mater. 26 (1990) 143–145 (in Russian).
[6] M. Jannin, C. Kolinsky, G. Godefroy, B. Jannot, N.I. Sorokina, D.Y. Lee, V.I. Simonov, V.I. Voronkova, V.K. Yanovskii, Eur. J. Solid State Inorg. Chem. 33 (1996) 607–621.
[7] N.I. Sorokina, V.I. Voronkova, V.K. Yanovskii, D.Y. Lee, M. Jannin, C. Kolinsky, G. Godefroy, B. Jannot, V.I. Simonov, Crystallogr. Rep. (Kristallografiya) 42 (1997) 39–45.
[8] D.Y. Lee, N.I. Sorokina, V.I. Voronkova, V.K. Yanovskii, I.A. Verin, V.I. Simonov, Crystallogr. Rep. (Kristallografiya) 42 (1997) 218–225.
[9] W.T.A. Harrison, M.L.F. Phillips, G.D. Stucky, Chem. Mater. 9 (1997) 1138–1144.
[10] P.A. Thomas, R. Duhlev, S.J.A. Teat, Acta Crystallogr. B50 (1994) 538–543.
[11] W.T.A. Harrison, M.L.F. Phillips, G.D. Stucky, Z. Kristallogr. 210 (1995) 295–297.
[12] J. Wang, J. Wei, Y. Liu, X. Yin, X. Hid, Z. Shao, M. Jiang, Prog. Crystal Growth Characterization Mater. 40 (2000) 3–15.
[13] N.I. Sorokina, V.I. Voronkova, V.K. Yanovskii, I.A. Verin, V.I. Simonov, Kristallografiya 41 (1996) 432–435.
[14] D.Y. Zhang, H.Y. Shen, W. Liu, W.Z. Chen, G.F. Zang, G. Zang, R.R. Zeng, C.H. Huang, W.X. Lin, J.K. Liang, J. Cryst. Growth 218 (2000) 98–102.
[15] G. Zhang, D. Zhang, H. Shen, W. Liu, C. Huang, L. Huang, Y. Wei, Opt. Commun. 241 (2004) 503–506.
[16] I. Koseva, V. Nikolov, P. Peshev, J. Alloys Compd. 353 (2003) L1–L4.
[17] M.L.F. Phillips, W.T.A. Harrison, T.E. Gier, G.D. Stucky, G.V. Kulkarni, J.K. Burdett, Inorg. Chem. 29 (1990) 2158–2163.
[18] O.D. Krotova, N.I. Sorokina, I.A. Verin, V.I. Voronkova, V.K. Yanovskii, V.I. Simonov, Crystallogr. Rep. (Kristallografiya) 48 (2003) 925–932.
[19] P.A. Thomas, S.C. Mayo, B.E. Watts, Acta Crystallogr. B48 (1992) 401–407.
[20] M. Abrabri, M. Rafiq, A. Larbot, J. Durand, J. Chim. Phys. Phys.–Chim. Biol. 92 (1995) 104–119.
[21] S.J. Crennell, A.K. Cheetham, R.H. Jarman, R.J. Thrash, J.A. Kaduk, J. Mater. Chem. 2 (1992) 383–386.
[22] E.M. McCarron III, J.C. Calabrese, T.E. Gier, J. Solid State Chem. 102 (1993) 354–361.
[23] K.K. Rangan, A. Verbaere, J. Gopalakrishnan, Mater. Res. Bull. 33 (1998) 395–399.
[24] A.A. Babaryk, I.V. Zatovsky, V.N. Baumer, N.S. Slobodyanik, O.V. Shishkin, Acta Crystallogr. C62 (2006) i91–i93.
[25] Oxford Diffraction. CrysAlis CCD and CrysAlis RED. Versions 1.171.28p4beta release (11-11-2005 CrysAlis 171.NET), Oxford Diffraction, Ltd. Abington, Oxfordshire, England, 2005.
[26] G.M. Sheldrick, SHELXS-97, University of Göttingen, Germany, 1997.
[27] G.M. Sheldrick, SHELXL-97. Program for crystal structure refinement, University of Göttingen, Germany, 1997.
[28] L.K. Cheng, J.D. Bierlein, J. Cryst. Growth 110 (1991) 697–703.
[29] A. Benabbas, M.M. Borel, A. Grandin, A. Leclaire, B. Raveau, Eur. J. Solid State Inorg. Chem. 29 (1992) 473–483.
[30] S. Deniard-Courant, Y. Piffard, M. Tournoux, Rev. Chim. Miner. 24 (1987) 276–287.
[31] O.A. Alekseeva, N.I. Sorokina, I.A. Verin, T.Yu. Losevskaya, V.I. Voronkova, V.K. Yanovskii, V.I. Simonov, Crystallogr. Rep. (Kristallografiya) 46 (2001) 816–822.
[32] O.A. Alekseeva, N.I. Sorokina, M.K. Blomberg, I.A. Verin, T.Yu. Losevskaya, V.I. Voronkova, V.K. Yanovskii, V.I. Simonov, Crystallogr. Rep. (Kristallografiya) 46 (2001) 215–220.

[33] D.E.C. Corbridge, Phosphorus. An Outline of its Chemistry, Biochemistry and Technology, vol. 2, second ed., Elsevier, Amsterdam–Oxford–New York, 1980.
[34] U. Peuchert, L. Bohaty, J. Schreuer, Acta Crystallogr. C53 (1997) 11–14.
[35] U. Peuchert, L. Bohaty, R. Froehlich, Acta Crystallogr. C51 (1995) 1719–1721.
[36] P.G. Nagornyi, A.A. Kapshuk, N.V. Stus', N.S. Slobodyanik, Kristallografiya 35 (1990) 634–637 (in Russian).
[37] K.-H. Lii, J. Chem. Soc. Dalton Trans. (1996) 815–818.
[38] S.T. Norberg, N. Ishizawa, Acta Crystallogr. C61 (2005) i99–i102.
[39] A.B.P. Lever, Inorganic Electronic Spectroscopy, second ed., Elsevier Science Publishers B.V., Amsterdam, 1984.